Liquid Crystals
Publication details, including instructions for authors and subscription information:
http://www.tandfonline.com/loi/tlct20

Synthesis and self-assembled nanostructures of novel chiral amphiphilic liquid crystals containing β-d-galactopyranoside end-groups

Ming-Shou Ho [a] & Chain-Shu Hsu [a]
[a] Department of Applied Chemistry , National Chiao Tung University , Hsinchu, Taiwan, 30010, Republic of China
Published online: 04 Mar 2010.

To cite this article: Ming-Shou Ho & Chain-Shu Hsu (2010) Synthesis and self-assembled nanostructures of novel chiral amphiphilic liquid crystals containing β-d-galactopyranoside end-groups, Liquid Crystals, 37:3, 293-301, DOI: 10.1080/02678291003611342

To link to this article: http://dx.doi.org/10.1080/02678291003611342

Liquid Crystals,
Vol. 37, No. 3, March 2010, 293–301

Taylor & Francis
Taylor & Francis Group

Synthesis and self-assembled nanostructures of novel chiral amphiphilic liquid crystals containing β-D-galactopyranoside end-groups

Ming-Shou Ho and Chain-Shu Hsu*

Department of Applied Chemistry, National Chiao Tung University, Hsinchu, Taiwan 30010, Republic of China

(Received 2 November 2009; final version received 11 January 2010)

A series of novel chiral amphiphilic liquid crystals that contain β-D-galactopyranoside end-group and 4-[1,2,3]-triazolephenyl 4-alkoxybenzoate mesogens were synthesised. Their phase transitions and mesomorphic properties were characterised by polarising optical microscopy and differential scanning calorimetry. All compounds obtained exhibit a chiral smectic A phase. In addition, the self-assembling behaviour in the solution of these liquid crystal amphiphiles that exhibited high segregation strength for phase separation was studied by electron microscopy. The morphological transformation of self-assembled chiral amphiphilic liquid crystals, from a platelet-like morphology to helical twists, was obtained by increasing the length of the hydrophobic alkyl tail.

Keywords: amphiphilic liquid crystals; heterocyclic liquid crystals; self-assembly; triazole

1. Introduction

Heterocyclic material, an interesting class of liquid crystal (LC), revealed highly promising ranges for a diverse group of niche applications. These compounds exhibited mesomorphic [1–9] and luminescent peculiarities [10–13]. Heterocyclic compounds, such as five-membered heterocyclic oxadiazole, thiophene and thiodiazole rings, were synthesised and characterised [14–16]. The detailed properties of an oxadiazole fragment were reported [17]. These compounds showed low transition temperature and wide LC range.

N-heterocyclic triazole compounds, albeit made synthetically, appeared to have widespread use in biological activities [18, 19]. In addition, application of the triazole ring in material chemistry, as organic light emitting devices as such, has been elucidated and demonstrated by Wang and Barnhill [20] and Choy *et al.* [21]. An efficient route to triazole-based dendrimers was recently investigated and reported by Wu *et al.* [22]. The triazole moiety possessed a quick and convenient aspect that could be utilised as a linkage for block copolymers [23]. Huisgen's dipolar cycloaddition of organic azides and alkynes provided a methodology for the most direct route to [1,2,3]-triazoles [24], and this most expedient method to form a five-membered heterocyclic ring is the so-called 'click reaction' [25,26]. The detailed mechanism of click cycloaddition was reported in detail by Fahmi *et al.* [27].

Accordingly to date, the [1,2,3]-triazole ring utilised in LC studies is rare, except for the few examples that contain the regioisomeric [1,2,4]-triazole [28–30] and syntheses reported by several groups [31–33], in which the triazole ring is used as a linkage between the aliphatic chiral material and a rigid core unity, which enables the materials to show smectic A and cholesteric mesophases, in which the molecules form helical macrostructures with a specific handedness.

Amphiphilic glycolipid molecules consist of hydrophilic (polar) head groups and hydrophobic (apolar) alkyl chains. Due to their polar asymmetry, the head groups and the alkyl chains self-aggregate into microscopic regions forming LC phases. They also exhibit amphotropic behaviour [34] in that they generate LC phases both in solvents as the concentration is varied and in their pure form as the temperature is varied. The LC phases produced in an aqueous medium are of great interest, in particular because of the role they play in biological cell membranes [35]. Both lyotropic and thermotropic properties of glycolipids have been widely studied in the last decade [36, 37].

Thermotropic LC phases of glycolipids were first observed in alkyl glucopyranosides, for example hexadecyl-β-D-glucopyranosides [38]. They are known to form smectic phases, which are believed to be similar or identical to the lamellar phase formed in an aqueous medium. The measured layer spacing indicated the formation of double layers. It is generally accepted that the hydrogen bond-forming ability of the polar moiety is crucial to the formation of mesophases in amphiphilic derivatives [39].

Self-assembling modified derivatives of naturally occurring monosaccharides provide a crucial direction for the controlled fabrication of superstructures. Shinkai *et al.* have made the most extensive use of sugars in their quest for organic hydrogelators. The

*Corresponding author. Email: cshsu@mail.nctu.edu.tw

ISSN 0267-8292 print/ISSN 1366-5855 online

DOI: 10.1080/02678291003611342
http://www.informaworld.com

morphologies of sugar-based amphiphiles, affected by the introduction of different hydrophilic or hydrophobic parts [40–44] and by unsaturation in the lipophilic moiety, have been thoughtfully studied by Shimizu and co-workers [45, 46]. The self-assembly of unsaturated alkyl chains of carbohydrate sugars exhibited an interesting self-assembled conversion from coiled nanofibres gradually to a tubular morphology. Recently, we reported some LC sugar-based rod–coil amphiphiles with different alkoxyl chain lengths that were self-assembled in solution to form either a platelet-like or a helical twist morphology [47–49].

In this study, a chiral β-D-galactopyranoside entity was linked to 4-[1,2,3]-triazolephenyl 4-alkoxybenzoate mesogen via click chemistry. The mesomorphic properties of the synthesised LCs are discussed. Furthermore, the self-assembling morphology of these chiral amphiphilic LCs in dilute solution was also investigated.

2. Experimental

2.1 Characterisation techniques

^{1}H nuclear magnetic resonance (NMR) spectra (300 MHz) were recorded on a Varian VXR-300 spectrometer. Thermal transitions and thermodynamic parameters were determined by using a Seiko SSC/6200 differential scanning calorimeter equipped with a liquid nitrogen cooling accessory. Heating and cooling rates were 5°C/min. Transition temperatures reported here were collected during the first heating and cooling scans. A Carl Zeiss Axiphot optical polarising microscope equipped with a Mettler FP 82 hot stage and a FP 80 central processor was used to observe the thermal transitions and analyse the anisotropic textures.

2.2 Materials

1-(3-Dimethylaminopropyl)-3-ethylcarbodiimide hydrochloride (EDCI) and 4-dimethylaminopyridine (DMAP) (from Aldrich) were used as received. The solvents were dried according to standard procedures. Tetrahydrofuran (THF) was distilled under a nitrogen atmosphere over sodium benzophenone ketyl just before use. Dichloromethane (DCM) and toluene were dried over calcium hydride and then distilled under nitrogen. Triethylamine (Et_3N) was distilled and dried over potassium hydroxide. Compound **1** and **3a**–**3f** were synthesised according to literature procedures [50, 51].

2.3 Synthesis of chiral amphiphilic LCs (LC7–LC12)

The synthetic processes of a series of chiral amphiphilic LCs (**LC7**–**LC12**) were outlined in Scheme 1. The detail procedures are described below.

2.3.1 4-(Trimethylsilyl ethynyl)phenol (2)

4-Iodophenol (10.0 g, 45.45 mmol), bis(tripheny1phosphine) palladium dichloride ($PdCl_2(PPh_3)_2$] (0.64 g, 0.91 mmol), CuI (0.69 g, 3.64 mmol), and PPh_3 (0.95 g, 3.64 mmol) were dissolved in Et_3N (150 ml) and the mixture was stirred under nitrogen. Once all catalysts had been dissolved, (trimethylsilyl) acetylene (9.6 ml, 68.18 mmol) was added. The resulting solution was reacted at 70°C for 15 h. After triethylamine was removed under reduced pressure, the product was extracted with diethyl ether. The crude product was isolated by evaporating the solvent and purified by column chromatography (silica gel, ethyl acetate/*n*-hexane = 1/4 as eluent) which afforded white crystals in 60% yield (5.19 g). ^{1}H NMR ($CDCl_3$): $\delta = 7.33$ (d, 2H, $J = 8.70$ Hz, aromatic protons), 6.73 (d, 2H, $J =$ 8.70 Hz, aromatic protons), 4.91 (s, 1H, –OH), 0.21 (s, 9H, $-Si(CH_3)_3$). ^{13}C NMR ($CDCl_3$): $\delta = 156.03$, 133.66, 115.32, 115.24, 105.13, 92.36, 0.02. mass spectrometry (MS) (EI): 190.

2.3.2 4-(Trimethylsilyl ethynyl)phenyl 4-alkoxybenzate (4a– 4f)

Both compounds were prepared by esterification of 4-alkoxybenzoic acid with 4-(trimethylsilyl ethynyl) phenol. An example for the synthesis of compound **4c** is described as follows.

A solution of EDCI (4.23 g, 22.07 mmol) in DCM (50 ml) was added dropwise to a solution of **2** (3.5 g, 18.39 mmol), 4-(nonyloxy)benzoic acid (**3c,** 5.8 g, 22.07 mmol) and DMAP (0.29 g, 2.39 mmol) in dichloromethane (100 ml) at −20°C. After complete addition, the reaction mixture was allowed to stir overnight at room temperature. The reaction progress was monitored by thin layer chromatography (TLC). The reaction mixture was washed twice with a 1 M sodium hydroxide solution and twice with distilled water. The organic layer was dried with anhydrous magnesium sulphate and then evaporated under reduced pressure to give the crude product. Further purification was performed using column chromatography (silica gel, ethyl acetate/*n*-hexane = 1/8 as eluent) to give a white solid (6.58 g, 82%). ^{1}H NMR ($CDCl_3$): $\delta = 8.10$ (d, 2H, $J = 8.70$ Hz, aromatic protons), 7.49 (d, 2H, $J = 8.70$ Hz, aromatic protons), 7.13 (d, 2H, $J = 8.70$ Hz, aromatic protons), 6.94 (d, 2H, $J = 9.0$ Hz, aromatic protons), 4.02 (t, 2H, $J =$ 6.60 Hz, $-PhOCH_2-$), 1.80 (m, 2H, $-PhOCH_2CH_2-$), 1.45–1.27 (m, 12H, $-(CH_2)_6CH_3$), 0.87 (t, 3H, $J = 6.30$ Hz, $-CH_2CH_3$), 0.23 (s, 9H, $-Si(CH_3)_3$). MS (EI): 436.

4a: Yield 85%. ^{1}H NMR ($CDCl_3$): $\delta = 8.10$ (d, 2H, $J = 9.30$ Hz, aromatic protons), 7.49 (d, 2H, $J = 8.70$ Hz, aromatic protons), 7.13 (d, 2H, $J = 9.00$ Hz,

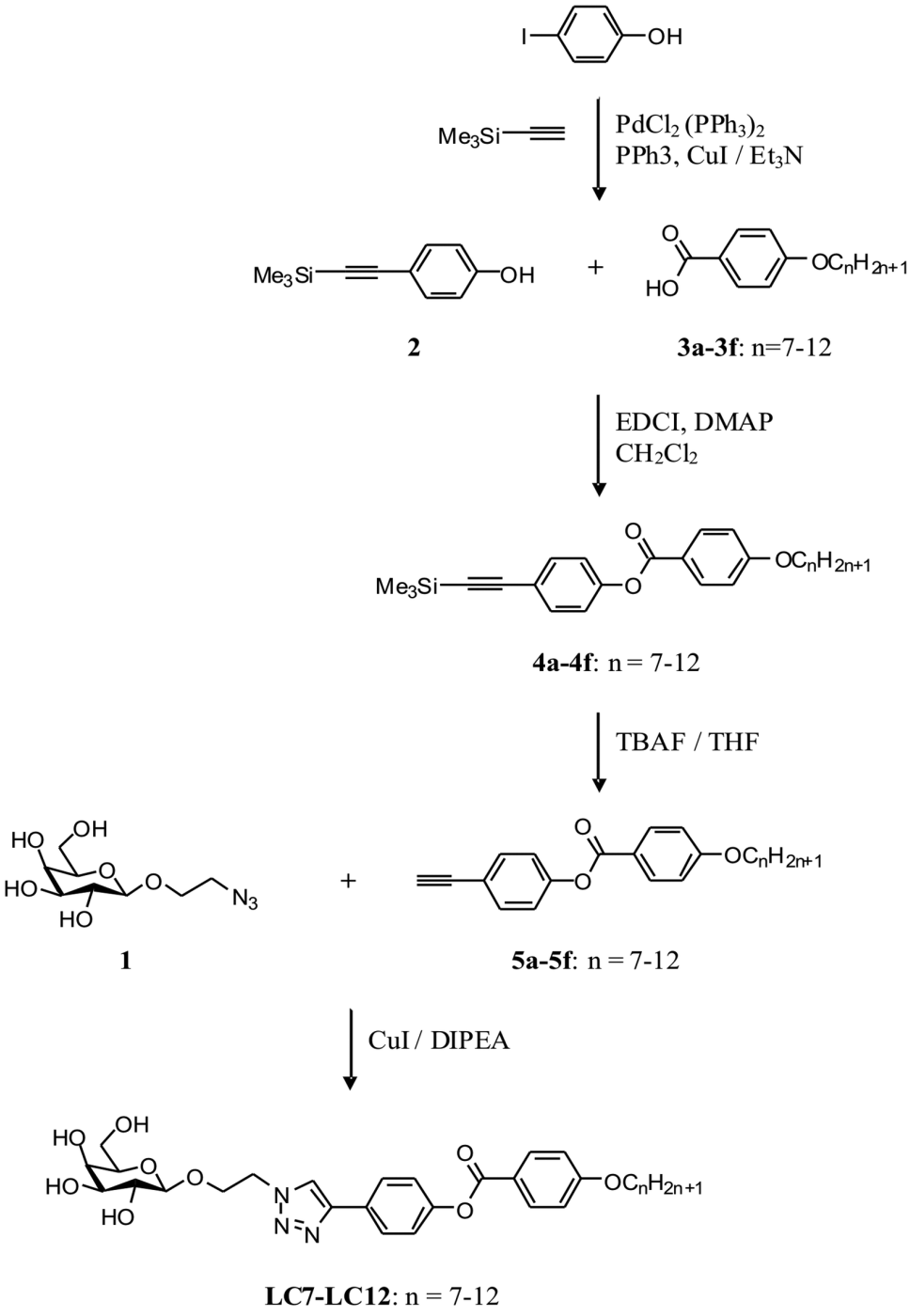

Scheme 1. Synthesis of the chiral amphiphilic liquid crystals (LC7–LC12).

aromatic protons), 6.94 (d, 2H, $J = 9.3$ Hz, aromatic protons), 4.02 (t, 2H, $J = 6.60$ Hz, –$PhOCH_2$–), 1.80 (m, 2H, –$PhOCH_2CH_2$–), 1.45–1.25 (m, 8H, –$(CH_2)_4CH_3$), 0.86 (t, 3H, $J = 6.30$ Hz, –CH_2CH_3), 0.23 (s, 9H, –$Si(CH_3)_3$). MS (EI): 408.

4b: Yield 90%. ^{1}H NMR ($CDCl_3$): $\delta = 8.10$ (d, 2H, $J = 8.70$ Hz, aromatic protons), 7.49 (d, 2H, $J = 8.40$ Hz, aromatic protons), 7.13 (d, 2H, $J = 8.40$ Hz, aromatic protons), 6.94 (d, 2H, $J = 8.7$ Hz, aromatic protons), 4.02 (t, 2H, $J = 6.60$ Hz, –$PhOCH_2$–), 1.80 (m, 2H, –$PhOCH_2CH_2$–), 1.45–1.21 (m, 10H, –$(CH_2)_5CH_3$), 0.87 (t, 3H, $J = 6.30$ Hz, –CH_2CH_3), 0.23 (s, 9H, –$Si(CH_3)_3$). MS (EI): 422.

4d: Yield 87%. ^{1}H NMR ($CDCl_3$): $\delta = 8.10$ (d, 2H, $J = 9.00$ Hz, aromatic protons), 7.49 (d, 2H, $J = 8.10$ Hz, aromatic protons), 7.13 (d, 2H, $J = 8.40$ Hz, aromatic protons), 6.94 (d, 2H, $J = 9.0$ Hz, aromatic protons), 4.02 (t, 2H, $J = 6.60$ Hz, –$PhOCH_2$–), 1.80 (m, 2H, –$PhOCH_2CH_2$–), 1.45–1.26 (m, 14H, –$(CH_2)_7CH_3$), 0.86 (t, 3H, $J = 6.30$ Hz, –CH_2CH_3), 0.23 (s, 9H, –$Si(CH_3)_3$). MS (EI): 450.

4e: Yield 87%. ^{1}H NMR ($CDCl_3$): $\delta = 8.10$ (d, 2H, $J = 9.00$ Hz, aromatic protons), 7.49 (d, 2H, $J = 8.70$ Hz, aromatic protons), 7.13 (d, 2H, $J = 8.40$ Hz, aromatic protons), 6.94 (d, 2H, $J = 9.30$ Hz, aromatic protons), 4.02 (t, 2H, $J = 6.60$ Hz, –$PhOCH_2$–), 1.80 (m, 2H, –$PhOCH_2CH_2$–), 1.41–1.25 (m, 16H, –$(CH_2)_8CH_3$), 0.86 (t, 3H, $J = 6.30$ Hz, –CH_2CH_3), 0.23 (s, 9H, –$Si(CH_3)_3$). MS (EI): 464.

4f: Yield 90%. ^{1}H NMR ($CDCl_3$): $\delta = 8.10$ (d, 2H, $J = 8.70$ Hz, aromatic protons), 7.49 (d, 2H, $J = 8.70$ Hz, aromatic protons), 7.13 (d, 2H, $J = 8.40$ Hz, aromatic protons), 6.94 (d, 2H, $J = 8.70$ Hz, aromatic protons), 4.02 (t, 2H, $J = 6.30$ Hz, –$PhOCH_2$–), 1.80 (m, 2H, –$PhOCH_2CH_2$–), 1.45–1.25 (m, 18H, –$(CH_2)_9CH_3$), 0.86 (t, 3H, $J = 6.30$ Hz, –CH_2CH_3), 0.24 (s, 9H, –$Si(CH_3)_3$). MS (EI): 478.

*2.3.3 4-Ethynylphenyl 4-alkoxybenzate (**5a–5f**)*

Both compounds were prepared by effected desilylation of compounds **4a–4f** with tetrabutylammonium fluoride (TBAF). An example for the synthesis of **5c** is described as follows.

TBAF (18 ml, 1 M/THF, 18 mmol) was added to a stirred solution of compound **4c** (5.24 g, 12 mmol) in THF (4 ml) at ambient temperature. The reaction mixture was stirred for 1hr, volatiles were evaporated, and the brown residue was partitioned (CH_2Cl_2/$NaHCO_{3\ (aq)}$). The organic layer was washed (brine), dried ($MgSO_4$), and evaporated. The residue was purified by column chromatography (ethyl acetate/*n*-hexane = 1/8) to give white crystals **5c** (2.26 g, 52%). ^{1}H NMR ($CDCl_3$): $\delta = 8.11$ (d, 2H, $J = 8.40$ Hz, aromatic protons), 7.53 (d, 2H, $J = 8.10$ Hz, aromatic protons), 7.16 (d, 2H, $J = 8.10$ Hz, aromatic protons), 6.95 (d, 2H, $J = 8.70$ Hz, aromatic protons), 4.02 (t, 2H, $J = 6.60$ Hz, –$PhOCH_2$–), 3.05 (s, 1H, –C≡CH), 1.80 (m, 2H, –$PhOCH_2CH_2$–), 1.46–1.25 (m, 12H, –$(CH_2)_6CH_3$), 0.86 (t, 3H, $J = 6.30$ Hz, –CH_2CH_3). MS (EI): 364.

5a: Yield 50%. ^{1}H NMR ($CDCl_3$): $\delta = 8.11$ (d, 2H, $J = 9.00$ Hz, aromatic protons), 7.53 (d, 2H, $J = 8.40$ Hz, aromatic protons), 7.16 (d, 2H, $J = 8.70$ Hz, aromatic protons), 6.95 (d, 2H, $J = 9.00$ Hz, aromatic protons), 4.02 (t, 2H, $J = 6.30$ Hz, –$PhOCH_2$–), 3.06 (s, 1H, –C≡CH), 1.80 (m, 2H, –$PhOCH_2CH_2$–), 1.41–1.23 (m, 8H, –$(CH_2)_4CH_3$), 0.88 (t, 3H, $J = 6.30$ Hz, –CH_2CH_3). MS (EI): 336

5b: Yield 50%. ^{1}H NMR ($CDCl_3$): $\delta = 8.10$ (d, 2H, $J = 8.70$ Hz, aromatic protons), 7.50 (d, 2H, $J = 8.50$ Hz, aromatic protons), 7.15 (d, 2H, $J = 8.50$ Hz, aromatic protons), 6.94 (d, 2H, $J = 8.7$ Hz, aromatic protons), 4.02 (t, 2H, $J = 6.60$ Hz, –$PhOCH_2$–), 3.06 (s, 1H, –C≡CH), 1.80 (m, 2H, –$PhOCH_2CH_2$–), 1.45–1.21 (m, 10H, –$(CH_2)_5CH_3$), 0.87 (t, 3H, $J = 6.30$ Hz, –CH_2CH_3). MS (EI): 350

5d: Yield 55%. ^{1}H NMR ($CDCl_3$): $\delta = 8.10$ (d, 2H, $J = 8.40$ Hz, aromatic protons), 7.52 (d, 2H, $J = 8.70$ Hz, aromatic protons), 7.16 (d, 2H, $J = 8.70$ Hz, aromatic protons), 6.95 (d, 2H, $J = 9.00$ Hz, aromatic protons), 4.02 (t, 2H, $J = 6.60$ Hz, –$PhOCH_2$–), 3.05 (s, 1H, –C≡CH), 1.80 (m, 2H, –$PhOCH_2CH_2$–), 1.45–1.26 (m, 14H, –$(CH_2)_7CH_3$), 0.86 (t, 3H, $J = 6.00$ Hz, –CH_2CH_3). MS (EI): 378

5e: Yield 60%. ^{1}H NMR ($CDCl_3$): $\delta = 8.11$ (d, 2H, $J = 8.70$ Hz, aromatic protons), 7.53 (d, 2H, $J = 8.70$ Hz, aromatic protons), 7.16 (d, 2H, $J = 8.40$ Hz, aromatic protons), 6.95 (d, 2H, $J = 8.70$ Hz, aromatic protons), 4.02 (t, 2H, $J = 6.60$ Hz, –$PhOCH_2$–), 3.06 (s, 1H, –C≡CH), 1.80 (m, 2H, –$PhOCH_2CH_2$–), 1.46–1.26 (m, 16H, –$(CH_2)_8CH_3$), 0.87 (t, 3H, $J = 6.30$, –CH_2CH_3). MS (EI): 392.

5f: Yield 62%. ^{1}H NMR ($CDCl_3$): $\delta = 8.11$ (d, 2H, $J = 9.00$ Hz, aromatic protons), 7.53 (d, 2H, $J = 8.70$ Hz, aromatic protons), 7.16 (d, 2H, $J = 8.70$ Hz, aromatic protons), 6.95 (d, 2H, $J = 9.00$ Hz, aromatic protons), 4.02 (t, 2H, $J = 6.60$ Hz, –$PhOCH_2$–), 3.06 (s, 1H, –C≡CH), 1.80 (m, 2H, –$PhOCH_2CH_2$–), 1.46–1.25 (m, 18H, –$(CH_2)_9CH_3$), 0.86 (t, 3H, $J = 6.30$, –CH_2CH_3). MS (EI): 406.

*2.3.4 Chiral amphiphilic LCs (**LC7–LC12**)*

Both compounds were prepared by using as a crucial step the Huisgen Cu(I)-catalysed cycloaddition of organic azido-galactose (**1**) with 4-ethynylphenyl 4-alkoxybenzates. An example for the synthesis of **LC9** is described as follows.

Compound **1** (1.22 g, 4.88 mmol), compound **5c** (1.78 g, 4.88 mmol) and CuI (4.65 g, 24.42 mmol) were dissolved in dry THF in a glass vial. To this mixture was added diisopropylethylamine (DIPEA, 8.4 ml, 48.84 mmol) and the vial was capped. After stirring for 24 h at room temperature, the mixture was filtered over Celite and the solvent evaporated under reduced pressure. The resulting residue was purified by flash chromatography using as eluent the gradient EtOAc/MeOH : EtOAc = 1:4). The title compound was isolated white crystals in 80% yield (2.4 g). ^{1}H NMR (DMSO–d_6): $\delta = 8.65$ (s, 1H, –C_2N_3H–), 8.07 (d, 2H, $J = 9.00$ Hz, aromatic protons), 7.92 (d, 2H, $J = 8.40$

Hz, aromatic protons), 7.33 (d, 2H, J = 8.70 Hz, aromatic protons), 7.11 (d, 2H, J = 8.70 Hz, aromatic protons), 5.06 (d, 1H, J = 4.80 Hz), 4.77 (d, 1H, J = 5.40 Hz), 4.60 (m, 3H), 4.35 (d, 1H, J = 4.80 Hz), 4.20 (d, 1H, J = 7.20 Hz), 4.08 (m, 3H), 3.90 (m, 1H), 3.62 (m, 1H), 3.50 (m, 1H), 1.74 (m, 2H, –$PhOCH_2CH_2$–), 1.42–1.25 (m, 12H, –$(CH_2)_6CH_3$), 0.85 (t, 3H, J = 5.70, –CH_2CH_3). ^{13}C NMR (DMSO–d_6): δ = 164.23, 163.25, 150.19, 145.57, 132.05, 128.62, 126.22, 122.50, 122.36, 120.74, 114.68, 103.41, 75.41, 73.35, 70.47, 68.14, 68.00, 67.18, 60.48, 49.81, 31.34, 29.11, 28.97, 28.74, 28.51, 25.42, 22.14, 13.97. MALDI-TOF: 614.301 $[M+H]^+$. HRMS (*m*/*z*) Calcd for $C_{32}H_{43}N_3O_9$: 613.6985, found: 613.6979.

LC7: Yield 82%. ^{1}H NMR (DMSO–d_6): δ = 8.66 (s, 1H, –C_2N_3H–), 8.07 (d, 2H, J = 8.70 Hz, aromatic protons), 7.90 (d, 2H, J = 7.80 Hz, aromatic protons), 7.33 (d, 2H, J = 7.80 Hz, aromatic protons), 7.11 (d, 2H, J = 8.70 Hz, aromatic protons), 5.10 (d, 1H, J = 4.20 Hz), 4.78 (d, 1H, J = 4.80 Hz), 4.61 (m, 3H), 4.40 (d, 1H, J=4.20 Hz), 4.19 (d, 1H, J = 6.60 Hz), 4.07 (m, 3H), 3.89 (m, 1H), 3.62 (m, 1H), 3.50 (m, 1H), 1.73 (m, 2H, –$PhOCH_2CH_2$–), 1.41–1.23 (m, 12H, –$(CH_2)_6CH_3$), 0.84 (t, 3H, J = 5.70, –CH_2CH_3). ^{13}C NMR (DMSO–d_6): δ = 164.24, 163.26, 150.20, 145.59, 132.04, 128.60, 126.25, 122.51, 122.37, 120.75, 114.65, 103.43, 75.43, 73.33, 70.45, 68.15, 68.01, 67.16, 60.45, 49.82, 31.33, 29.12, 28.54, 25.42, 22.17, 13.96. MALDI-TOF: 586.269 $[M+H]^+$. HRMS (*m*/*z*) Calcd for $C_{30}H_{39}N_3O_9$: 585.6454, found: 585.6465.

LC8: Yield 85%. ^{1}H NMR (DMSO–d_6): δ = 8.66 (s, 1H, –C_2N_3H–), 8.07 (d, 2H, J = 8.70 Hz, aromatic protons), 7.90 (d, 2H, J = 8.40 Hz, aromatic protons), 7.33 (d, 2H, J = 8.40 Hz, aromatic protons), 7.11 (d, 2H, J = 8.70 Hz, aromatic protons), 5.09 (d, 1H, J = 4.80 Hz), 4.77 (d, 1H, J = 5.10 Hz), 4.60 (m, 3H), 4.39 (d, 1H, J = 4.20 Hz), 4.19 (d, 1H, J = 6.60 Hz), 4.08 (m, 3H), 3.90 (m, 1H), 3.62 (m, 1H), 3.50 (m, 1H), 1.74 (m, 2H, –$PhOCH_2CH_2$–), 1.41–1.26 (m, 12H, –$(CH_2)_6CH_3$), 0.85 (t, 3H, J = 5.70, –CH_2CH_3). ^{13}C NMR (DMSO–d_6): δ = 164.23, 163.26, 150.19, 145.59, 132.05, 128.60, 126.22, 122.51, 122.36, 120.75, 114.68, 103.43, 75.41, 73.33, 70.47, 68.15, 68.00, 67.16, 60.48, 49.82, 31.34, 29.12, 28.74, 28.53, 25.42, 22.15, 13.96. MALDI-TOF: 600.284 $[M+H]^+$. HRMS (*m*/*z*). Calculated for $C_{31}H_{41}N_3O_9$: 599.6719, found: 599.6729.

LC10: Yield 80%. ^{1}H NMR (DMSO–d_6): δ = 8.64 (s, 1H, –C_2N_3H–), 8.07 (d, 2H, J = 9.00 Hz, aromatic protons), 7.90 (d, 2H, J = 8.70 Hz, aromatic protons), 7.33 (d, 2H, J = 8.70 Hz, aromatic protons), 7.11 (d, 2H, J = 8.70 Hz, aromatic protons), 5.03 (d, 1H, J = 4.80 Hz), 4.71 (d, 1H, J = 5.10 Hz), 4.56 (m, 3H), 4.35 (d, 1H, J = 4.80 Hz), 4.20 (d, 1H, J = 7.20 Hz), 4.08 (m, 3H), 3.91 (m, 1H), 3.62 (m, 1H), 3.51 (m, 1H), 1.74 (m, 2H, –$PhOCH_2CH_2$–), 1.42–1.25 (m, 14H, –$(CH_2)_7CH_3$), 0.85 (t, 3H, J = 5.70, –CH_2CH_3). ^{13}C NMR (DMSO–d_6): δ = 164.20, 163.25, 150.20, 145.56, 132.03, 128.64, 126.25, 122.49, 122.35, 120.72, 114.69, 103.43, 75.43, 73.33, 70.46, 68.16, 68.03, 67.19, 60.46, 49.80, 31.35, 29.11, 28.97, 28.75, 28.64, 28.52, 25.45, 22.14, 13.99. MALDI-TOF: 628.230 $[M+H]^+$. HRMS (*m*/*z*) Calculated for $C_{33}H_{45}N_3O_9$: 627.7251, found: 627.7261.

LC11: Yield 85%. ^{1}H NMR (DMSO–d_6): δ = 8.66 (s, 1H, –C_2N_3H–), 8.07 (d, 2H, J = 9.00 Hz, aromatic protons), 7.90 (d, 2H, J = 8.70 Hz, aromatic protons), 7.33 (d, 2H, J = 8.70 Hz, aromatic protons), 7.11 (d, 2H, J = 9.00 Hz, aromatic protons), 5.09 (d, 1H, J = 4.80 Hz), 4.77 (d, 1H, J = 5.40 Hz), 4.60 (m, 3H), 4.39 (d, 1H, J = 4.50 Hz), 4.19 (d, 1H, J = 6.90 Hz), 4.08 (m, 3H), 3.89 (m, 1H), 3.62 (m, 1H), 3.50 (m, 1H), 1.73 (m, 2H, –$PhOCH_2CH_2$–), 1.41–1.24 (m, 16H, –$(CH_2)_8CH_3$), 0.85 (t, 3H, J = 5.70, –CH_2CH_3). ^{13}C NMR (DMSO–d_6): δ = 164.22, 163.25, 150.19, 145.56, 132.05, 128.64, 126.22, 122.49, 122.36, 120.72, 114.68, 103.43, 75.41, 73.33, 70.47, 68.16, 68.00, 67.19, 60.48, 49.80, 31.34, 29.10, 29.03, 28.97, 28.76, 28.64, 28.51, 25.44, 22.14, 13.98. MALDI-TOF: 642.331 $[M+H]^+$. HRMS (*m*/*z*) Calculated for $C_{34}H_{47}N_3O_9$: 641.7517, found: 641.7525.

LC12: Yield 90%. ^{1}H NMR (DMSO–d_6): δ = 8.65 (s, 1H, –C_2N_3H–), 8.07 (d, 2H, J = 8.70 Hz, aromatic protons), 7.90 (d, 2H, J = 8.40 Hz, aromatic protons), 7.33 (d, 2H, J = 8.70 Hz, aromatic protons), 7.11 (d, 2H, J = 9.00 Hz, aromatic protons), 5.08 (d, 1H, J = 4.50 Hz), 4.76 (d, 1H, J = 5.10 Hz), 4.60 (m, 3H), 4.39 (d, 1H, J = 4.80 Hz), 4.19 (d, 1H, J = 7.20 Hz), 4.08 (m, 3H), 3.90 (m, 1H), 3.62 (m, 1H), 3.50 (m, 1H), 1.73 (m, 2H, –$PhOCH_2CH_2$–), 1.42–1.23 (m, 18H, –$(CH_2)_9CH_3$), 0.84 (t, 3H, J = 5.40, –CH_2CH_3). ^{13}C NMR (DMSO–d_6): δ = 164.22, 163.24, 150.19, 145.55, 132.05, 128.65, 126.22, 122.48, 122.36, 120.70, 114.68, 103.45, 75.41, 73.34, 70.47, 68.17, 68.01, 67.19, 60.46, 49.80, 31.32, 29.10, 29.04, 29.03, 28.96, 28.76, 28.66, 28.51, 25.44, 22.13, 13.98. MALDI-TOF: 656.510 $[M+H]^+$. HRMS (*m*/*z*) Calculated for $C_{35}H_{49}N_3O_9$: 655.7783, found: 655.7793.

3. Results and discussion

3.1 Synthesis

We designed multistep reaction routes for the synthesis of chiral amphiphilic LCs as illustrated in Scheme 1. Hydrophilic head group was prepared using 2-azidoethyl-β-D-galacto-pyranoside (**1**) which was synthesised by glycosylation of β-D-galactose pentaacetate with 2-azidoethanol and further deprotection of acetyl protection groups. Hydrophobic rigid core of LC

molecules was constructed starting from 4-iodophenol by copper–palladium catalysed cross-coupling (Sonogashira–Tohda–Hagihara coupling) [52, 53] with (trimethylsilyl)acetylene followed by esterification with 4-alkoxybenzoic acid. Subsequently, desilylation of the trimethylsilyl protecting group appeared to be a convenient method to prepare the alkyne counterpart. Finally, the target chiral amphiphilic LCs with different alkyl chain lengths were prepared via copper(I)-catalysed regiospecific 1,3-cycloaddition. All obtained compounds were fully characterised by standard spectroscopic methods, from which satisfactory analysis data corresponding to their expected molecular structures were obtained.

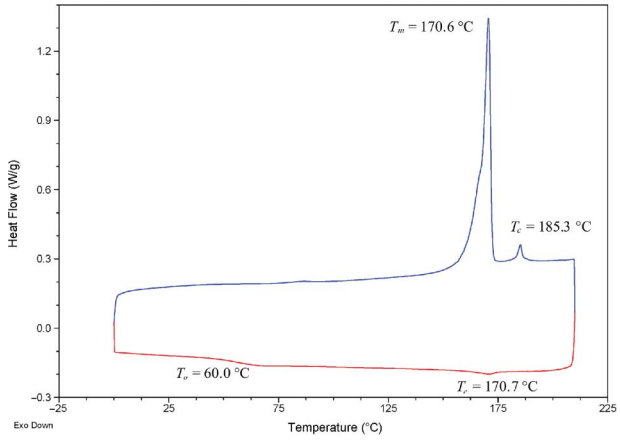

Figure 1. Differential scanning thermograms for the first heating and cooling cycle for LC12, scan rate 5°C min^{-1}.

3.2 Mesomorphic properties of LC7–LC12

Phase transition temperatures and mesophase texture of the chiral amphiphilic LCs were determined by a combination of polarising optical microscopy and differential scanning calorimetry (DSC) measurements.

Figure 1 depicts the representative DSC thermograms of **LC12**. A melting transition at 170.6°C and a smectic A to isotropic phase transition at 185.3°C are observed in the first heating scan. In the cooling scan, it displays an isotropic to smectic A phase transition at 170.7°C followed by a glass transition at 60°C. Figure 2 shows the photographs of a smectic A fan texture of LC amphiphiles. According to the literature [54–57], the saccharide-containing LCs always form a glassy state on the DSC scans. As the synthesised LC compounds contain a galactopyranoside chiral entity, they are possible to form chiral smectic A phase. We utilise optical microscopy to investigate their textures. When the LC compounds are melted into the LC phase, an oily-streak texture (Figure 2(c)) was produced and homeotropic areas were bounded by the streaks [54, 55]. Cooling from the isotropic phase generates what initially appears to be a chiral smectic A phase with regions of focal conic fan texture and regions of not completely black homeotropic texture. However, it is obvious that optically extinct homeotropic regions become even more evident on further cooling. This optically uniaxial is possibly due to the fact that the amphiphilic molecules adhere more to the surface of glass slides via hydrogen bonding when further cooled [56, 57]. Both chiral SmA and SmC phases possess focal–conic defects. However, only SmA phase can form a corresponding homeotropic texture. The coexisting presence of these two observations classifies the mesophase as smectic A. We believe the bend imposed

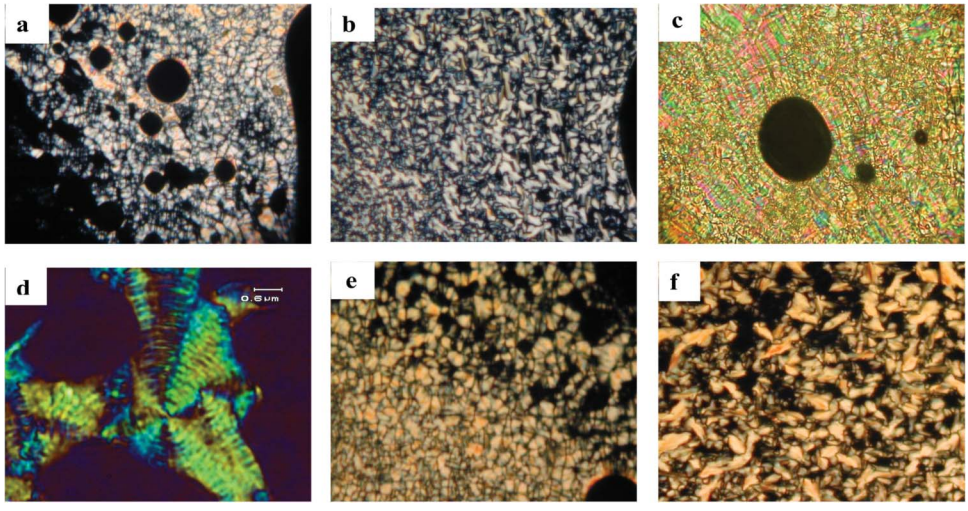

Figure 2. Polarised optical micrographs displayed by (a) LC7, (b) LC8, (c) LC9, (d) LC10, (e) LC11 and (f) LC12.

Table 1. The transition temperatures and associated enthalpies data for the chiral amphiphilic liquid crystals.

Compound	Melting point[a]		Clearing temperature[a]		Glass transition temperature[b]
	T/°C	ΔH/(J g^{-1})	T/°C	ΔH/(J g^{-1})	T/°C
LC7	132.3	37.11	157.9	4.75	70.4
LC8	153.1	50.35	179.8	2.79	65.2
LC9	168.0	79.59	186.8	1.01	72.4
LC10	161.3	59.86	189.5	0.12	70.8
LC11	166.3	83.27	196.2	0.58	68.8
LC12	170.6	65.65	185.3	2.29	60.0

Notes: [a]Data obtained by the differential scanning calorimetry (DSC) first heating scan.
[b]Data taken from the DSC first cooling scan.

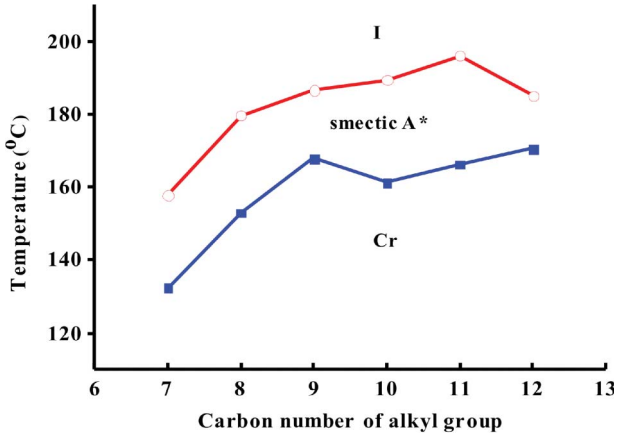

Figure 3. Melting (Tm, ■) and isotropisation (TSmA*, ○) temperatures of the chiral amphiphilic liquid crystals, as a function of the carbon number of the alkyl group.

by the triazole ring is so large that the effective polar packing necessary to build up a SmC is disrupted.

Figure 2(a) and (e) show the elliptical and hyperbolic lines of optical characterisation of focal–conic defects exhibited by the LC amphiphiles. These observations show that the LC phase is a chiral smectic A (SmA*) phase [58–60].

The enthalpies for the various transitions of the chiral amphiphilic LCs are given in Table 1. In addition, the glass transition temperatures are also given, as these were not able to be determined accurately from thermal optical microscopy. It is seen that increasing the terminal chain length results in the increasing of the smectic A*–isotropic liquid transition temperature T_{SmA*} (Figure 3). This shows clearly that steric factors and the ratio of the size of the hydrophilic head group to the hydrophilic hydrocarbon chain are much more important in determining the thermotropic mesomorphism of amphotropic compounds [61].

3.3 Self-assembled hierarchical superstructures in solution

The self-assembled morphology of the chiral amphiphilic LCs in solution was examined by field-emission scanning electron microscopy (FESEM) and transmission electron microscopy (TEM). An interesting morphological evolution was identified according to the change of the alkenyloxy chain length. At low alkoxyl chain length, the self-assembled morphology exhibited a platelet-like morphology. However, helical twists were identified once the alkoxyl chain length reached a certain value. The **LC10** amphiphile having 10 methylene units in the alkoxyl chain exhibited both platelet-like morphology and left-handed helical twists morphologies (Figure 4(a)), while both **LC11** and **LC12** containing longer alkoxyl chain length revealed only a left-handed helical twists morphology. It is also noted that the pitch length of the helical twists decreases with increasing alkoxyl chain length. These results are agreed with our previous investigation on the sugar-containing LC molecules [47–49]. The helicity of the LC molecules is primarily induced by the chiral galactopyranoside end group. However, the helicity is amplified in the LC state because rod segments π–π interaction leads to a liquid-crystalline-like aggregation that will stabilise the helical morphology.

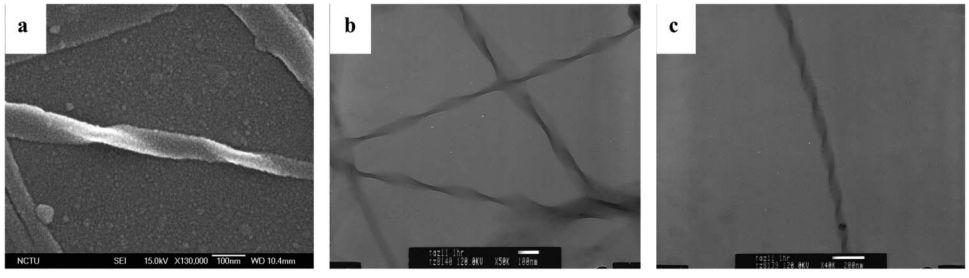

Figure 4. FESEM (left) and TEM micrographs of (a) LC10, (b) LC11, and (c) LC12 self-assembled morphologies in THF/H_2O solution.

4. Conclusion

In summary, we have prepared for the first time chiral amphiphilic LCs via Cu(I)-catalysed click reaction. All compounds were identified to exhibit a chiral smectic A phase. The self-assembling behaviour in the dilute solution of these chiral amphiphilic liquid crystals was investigated. The morphological transformation from a platelet-like morphology to helical twists was obtained by increasing the length of the hydrophobic alkoxy chain. The synthesised chiral amphiphilic liquid crystals that will aggregate to form helical superstructures have potential applications in optical switching and sensors devices.

Acknowledgements

The authors are grateful to the final support from National Science Council, Taiwan, Republic of China.

References

[1] Demus, D.; Goodby, G.; Gray, G.W.; Spiess, H.W.; Vill, V. *Handbook of Liquid Crystals*, vols. 1–3; Weinheim: Wiley-VCH, 1998.
[2] Vasconcelos, U.V.; Dalmolin, E.; Merlo, A.A. *Org. Lett.* **2005**, *7*, 1027–1030.
[3] Paraskos, A.J.; Swager, T.M. *Chem. Mater*. **2002**, *14*, 4543–4549.
[4] Mallia, A.; George, M.; Das, S. *Chem. Mater.* **1999**, *11*, 207–208.
[5] Aldred, M.P.; Vlachos, P.; Dong, D.; Kitney, S.P.; Tsoi, W.C.; O'Neill, M.; Kelly, S.M. *Liq. Cryst.* **2005**, *32*, 951–965.
[6] da Silva, L.; Gallardo, H.; Begnini, I.M.; Magnago, R. *Mol. Cryst. Liq. Cryst.* **2005**, *432*, 1–13.
[7] Sung, H-H.; Lin, H-C. *Liq. Cryst.* **2004**, *31*, 831–841.
[8] Chien, C.W.; Liu, K.T.; Lai, C.K. *Liq. Cryst.* **2004**, *31*, 1007–1017.
[9] Lee, C-H.; Yamamoto, T. *Mol. Cryst. Liq. Cryst.* **2001**, *363*, 77–84.
[10] Cristiano, R.; Vieira, A.A.; Ely, F.; Gallardo, H. *Liq. Cryst.* **2006**, *33*, 381–390.
[11] Cristiano, R.; Santos, D.M.P.O.; Gallardo, H. *Liq. Cryst.* **2005**, *32*, 7–14.
[12] Cristiano, R.; Ely, F.; Gallardo, H. *Liq. Cryst.* **2005**, *32*, 15–25.
[13] Lai, C.K.; Liu, H.C.; Li, F.J.; Cheng, K.L.; Sheu, H.S. *Liq. Cryst.* **2005**, *32*, 85–94.
[14] Sato, M.; Ishii, R.; Nakashima, S.; Yonetake, K.; Kido, J. *Liq. Cryst.* **2001**, *28*, 1211–1214.
[15] Parra, M.; Hidalgo, P.; Carrasco, E.; Barbera, J.; Silvino, L. *Liq. Cryst.* **2006**, *33*, 875–882.
[16] Seed, A.J.; Cross, G.J.; Toyen, K.J.; Goodby, J.W. *Liq. Cryst.* **2003**, *30*, 1089–1107.
[17] Karamysheva, L.A.; Torgova, S.I.; Agafonova, I.F.; Petrov, V.F. *Liq. Cryst.* **2000**, *27*, 393–405.
[18] Li, J.; Zhang, M.; Tang, W.; He, P.L.; Zhu, W.; Li, T.; Zuo, J.P.; Liu, H.; Jiang, H. *Bioorg. Med. Chem. Lett*. **2006**, *16*, 5009–5013.
[19] Alvarez, R.; Velazquez, S.; San-Felix, A.; Aquaro, S.; De Clercq, E.; Perno, C.F.; Karlsson, A.; Balzarini, J.; Camarasa, M.J. *J. Med. Chem.* **1994**, *37*, 4185–4194.
[20] Wang, Q.; Barnhill, H.N. *Org. Lett.* **2004**, *6*, 4603–4606.
[21] Choy, G.; Choyke, P.; Libutti, S.K. *Mol. Imaging* **2003**, *2*, 303–312.
[22] Wu, P.; Feldman, A.K.; Nugent, A.K.; Hawker, C.J.; Scheel, A.; Voit, B.; Pyun, J.; Frechet, J.M.J.; Sharpless, K.B.; Fokin, V.V. *Angew. Chem. Int. Ed.* **2004**, *43*, 3928–3932.
[23] Opsteen, J.A.; van Hest, J.C.M. *Chem. Comm.* **2005**, *1*, 57–59.
[24] Huisgen, R. In *1,3-Dipolar Cycloaddition Chemistry*; Padwa, A. ed.; New York: Wiley, 1984. pp. 1–176.
[25] Kolb, H.C.; Finn, M.G.; Sharpless, K.B. *Angew. Chem.* **2001**, *113*, 2056–2075.
[26] Kolb, H.C.; Finn, M.G.; Sharpless, K.B. *Angew. Chem. Int. Ed*. **2001**, *40*, 2004–2021.
[27] Fahmi, H.; Lovell, T.; Hilgraf, R.; Rostovtsev, V.V.; Noodleman, L.; Sharpless, K.B.; Fokin, V.V. *J. Am. Chem. Soc.* **2005**, *127*, 210–216.
[28] Fernández, O.; de la Torre, G.; Fernández-L, F.; Barberá, J.; Torres, T. *Chem. Mater.* **1997**, *9*, 3017–3022.
[29] Li, W-R.; Su, J-C.; Ke, Y-C.; Lai, C-K. *J. Mater. Chem.* **2001**, *11*, 1763–1765.
[30] Su, C.; Lee, L-X.; Yu, S-H.; Shih, Y-K.; Su, J-C.; Li, F-J.; Lai, C.K. *Liq. Cryst.* **2004**, *31*, 745–749.
[31] Cristiano, R.; Santos, D.M.P.; Conte, G.; Gallardo, H. *Liq. Cryst.* **2006**, *33*, 997–1003.
[32] Gallardo, H.; Ely, F.; Bortoluzzi, A.J.; Conte, G. *Liq. Cryst.* **2005**, *32*, 667–671.
[33] Conte, G.; Ely, F.; Gallardo, H. *Liq. Cryst.* **2005**, *32*, 1213–1222.
[34] Pfannemüller, B.; Welte, W.; Chin, E.; Goodby, J.W. *Mol. Cryst. Liq. Cryst*. **1986**, *1*, 357–370.
[35] Brown, G.H.; Walken, J.J. *Liquid Crystals and Biological Structures*. Academic Press: New York, 1979.
[36] Villand, V.; Hashim, R. *Curr. Opin. Colloid Interface Sci*. **2002**, *7*, 395–409.
[37] Goodby, J.W.; Görtz, V.; Cowling, S.J.; Mackenzie, G.; Martin, P.; Plusquellec, D.; Benvegnu, T.; Boullanger, P.; Lafont, D.; Queneau, Y.; Chambert, S.; Fitremann, J. *Chem. Soc. Rev*. **2007**, *36*, 1971–2032.
[38] Fischer, E.; Helferch, B. *Liebigs. Ann. Chem.* **1911**, *383*, 68–70.
[39] Vill, V.; Böcker, T.; Thiem, J.; Fischer, F. *Liq. Cryst.* **1989**, *6*, 349–356.
[40] Jenekhe, S.A.; Chen, X.L. *Science* **1998**, *279*, 1903–1907.
[41] Van Doren, H.A.; Smits, E.; Pestman, J.M.; Engberts, J.B.F.N.; Kellogg, R.M. *Chem. Soc. Rev.* **2000**, *29*, 183–199.
[42] Laurent, N.; Lafon, D.; Dumoulin, F.; Boullanger, P.; Mackenzie, G.; Kouwer, P.H J.; Goodby, J.W. *J. Am. Chem. Soc.* **2003**, *125*, 15499–15506.
[43] Jung, J.H.; Yoshida, K.; Shimizu, T. *Langmuir*, **2002**, *18*, 8724–8727.
[44] Shimizu, T.; Masuda, M.; Minamikawa, H. *Chem. Rev.* **2005**, *105*, 1401–1443.
[45] John, G.; Masuda, M.; Okada, Y.; Yase, K.; Shimizu, T. *Adv. Mater*. **2001**, *13*, 715–718.
[46] John, G.; Jung, J.H.; Minamikawa, H.; Yoshida, K.; Shimizu, T. *Chem. Eur. J.* **2002**, *8*, 5495–5500.
[47] Sung, C-H.; Kung, L-R.; Hsu, C-S.; Lin, T-F.; Ho, R-M. *Chem. Mater*. **2006**, *18*, 352–359.

[48] Lin, T-F.; Ho, R-M.; Sung, C-H.; Hsu, C-S. *Chem. Mater*. **2006**, *18*, 5510–5519.
[49] Lin, T-F.; Ho, R-M.; Sung, C-H.; Hsu, C-S. *Chem. Mater*. **2008**, *24*, 1404–1409.
[50] Fazio, F.; Bryan, M.C.; Blixt, O.; Paulson, J.C.; Wong, C-H. *J. Am. Chem. Soc.* **2002**, *124*, 14397–14402.
[51] Kutsumizu, S.; Mori, H.; Fukatami, M.; Naito, S.; Sakajiri, K.; Saito, K. *Chem. Mater.* **2008**, *20*, 3675–3687.
[52] Sonogashira, K.; Tohda, Y.; Hagihara, N. *Tetrahedron Lett.* **1975**, *16*, 4467–4470.
[53] Sonogashira, K. *J. Organomet. Chem*. **2002**, *653*, 46–49.
[54] Pfannemüller, B.; Welte, W.; Chin, E.; Goodby, J.W. *Liq. Cryst.* **2006**, *33*, 1229–1245.
[55] Demus, D.; Richter, L. *Textures of Liquid Crystals*. Verlag-Chemie.
[56] Goodby, J.W.; Haley, J.A.; Mackenzie, G.; Watson, M.J.; Plusquellec, D.; Ferrières. V. *J. Mater. Chem.* **1995**, *5*, 2209–2220.
[57] Gray, G.W.; Goodby, J.W. *Smectic Liquid Crystals*, Leonard-Hill, 1984.
[58] Bault, P.; Gode, P.; Goethals, G.; Goodby, J.W.; Haley, J.A.; Kelly, S.M.; Mehl, G.H.; Ronco, G.; Villa, P. *Liq. Cryst.* **1998**, *24*, 283–293.
[59] Goodby, J.W. *Mol. Cryst. Liq. Cryst.* **1984**, *110*, 205–219.
[60] Van Doren, H.A. Wingert, L.M. *Mol. Cryst. Liq. Cryst.* **1991**, *198*, 381–391.
[61] Letellier, P.; Ewing, D.F.; Goodby, J.W.; Haley, J.A.; Kelly, S.M.; Mackenzie, G. *Liq. Cryst.* **1997**, *22*, 609–620.